VELOCITY PROFILE OPTIMIZATION FOR THE RIGA DYNAMO EXPERIMENT

F. STEFANI AND G. GERBETH
Forschungszentrum Rossendorf
P.O. Box 510119, D-01314 Dresden, Germany

AND

A. GAILITIS
Institute of Physics, Latvian Academy of Sciences
LV-2169 Salaspils 1, Riga, Latvia

1. Introduction

The Riga dynamo experiment is intended to verify the self-excitation of a magnetic field in an electrically conducting fluid. Stimulated by the early work of Ponomarenko [1], the basic component of the facility consists of an axially symmetric helical flow of liquid sodium. In contrast to the Ponomarenko dynamo, this central helical flow is surrounded by a non-helical back-flow and an outermost cylinder filled with sodium at rest. This experimental arrangement enables not only a convective instability for the magnetic field excitation (as in the case of the Ponomarenko dynamo), but also an absolute instability [2].

Calculating the critical magnetic Reynolds numbers (Rm) for a given geometry under the assumption of solid body rotation in the innermost cylinder, Gailitis [3] estimated the sodium flow and the power supply necessary for magnetic field self-excitation.

However, a main problem of the Riga dynamo experiment arises from the strong dependence of the critical Rm on the shape of the velocity profiles and from the difficulty to generate a desirable flow by means of a propeller and suitable guiding blades[1]. For example, the velocity profiles measured in a water pre-experiment in 1996 turned out to differ widely from a solid

[1]This is in contrast to the Karlsruhe experiment, where the precise shape of the velocity profile plays only a negligible role due to the effect of scale separation [4].

body rotation [5].
In order to compute the critical Rm for these measured profiles and to look for profiles with critical Rm as low as possible, we carried out a number of numerical simulations. For the bulk of the calculations we used a finite difference solver for the time-dependent induction equation in one dimension (1D), taking into account only the first azimuthal component and fixed Fourier components in z-direction. Some of these results were verified by comparison with the outcomes of an eigenvalue equation solver. Additionally, a two-dimensional (2D) code was developed and used in order to check the effects of the finite length of the system and of possible variations of the velocity profiles along the z-axis.

2. Optimization Criterion

First water experiments at the Riga dynamo facility had shown a remarkable deviation of the measured velocity profiles from the solid body rotation profiles supposed in former calculations. At the same time, preliminary computations had indicated a strong dependence of the critical Rm on the shapes and the relative strengths of the azimuthal velocity v_ϕ and the axial velocity v_z. Thus, in order to achieve self-excitation for a given power supply, a change of the velocity profiles was unavoidable.
The first difficulty for a velocity profile optimization applies to the definition of a sensible optimization criterion. In a technical sense, it would be desirable to find velocity profiles which require minimal power for the self-excitation of a magnetic field. However, the determination of the necessary power would represent a difficult hydrodynamic task for its own. An easier task is to look for velocity profiles with a minimal critical Rm. But even the definition of Rm is to some extent arbitrary. Here we use the following definition:

$$Rm = \mu\sigma \; R_1 \sqrt{\overline{v_z{}^2} + 2\,\overline{v_\phi{}^2}}\;.$$

By virtue of the averaging

$$\overline{v_*{}^2} = \frac{2}{R_1^2} \int_0^{R_1} v_*{}^2(r)\, r dr$$

over the radius R_1 of the innermost cylinder, this definition has regard to the integral properties of the flow and not only to the maximal velocity. At the same time, for the special case of solid body rotation it is equivalent to the often used definition $Rm = \mu\sigma R_1 v_{max}$. According to our definition of Rm, we define the pitch parameter κ as

$$\kappa \;=\; \sqrt{\frac{\overline{v_z{}^2}}{2\,\overline{v_\phi{}^2}}}.$$

3. Basic equations and the numerical codes

Being interested only in the onset of the magnetic field excitation, we restrict ourselves to the kinematic problem. Further on, we assume the velocity profile to be axisymmetric:

$$\mathbf{v}(\mathbf{r}) = (v_r(r,z), v_\phi(r,z), v_z(r,z)).$$

(For the 1D code the v_r-component and the z-dependence of the remaining components are also neglected.) Combining Maxwell's equations and Ohm's law we find the induction equation for the magnetic field:

$$\frac{\partial \mathbf{B}}{\partial t} = -\frac{1}{\mu\sigma}\nabla\times(\nabla\times\mathbf{B}) + \nabla\times(\mathbf{v}\times\mathbf{B})\ .$$

It is well known [6], that for low Rm only the azimuthal mode with $m=1$ is excited; thus we can make the ansatz

$$\mathbf{B}(r,\phi,z,t) = \left(\tilde{B}_r(r,t), \tilde{B}_\phi(r,t), \tilde{B}_z(r,t)\right) exp(i\phi + ikz)$$

for the 1D code and

$$\mathbf{B}(r,\phi,z,t) = \left(\tilde{B}_r(r,z,t), \tilde{B}_\phi(r,z,t), \tilde{B}_z(r,z,t)\right) exp(i\phi)$$

for the 2D code. Then, for the 1D case, the induction equation can be written in the following form:

$$\begin{aligned}
\frac{\partial \tilde{B}_r(r,t)}{\partial t} &= \frac{1}{\mu\sigma}\left[\left(\frac{1}{r}\frac{\partial}{\partial r}r\frac{\partial}{\partial r} - \frac{1}{r^2} - \frac{m^2}{r^2} - k^2\right)\tilde{B}_r(r,t) - \frac{2im}{r^2}\tilde{B}_\phi(r,t)\right] \\
&\quad - \left(\frac{im}{r}v_\phi + ikv_z\right)\tilde{B}_r(r,t) \\
\frac{\partial \tilde{B}_\phi(r,t)}{\partial t} &= \frac{1}{\mu\sigma}\left[\left(\frac{1}{r}\frac{\partial}{\partial r}r\frac{\partial}{\partial r} - \frac{1}{r^2} - \frac{m^2}{r^2} - k^2\right)\tilde{B}_\phi(r,t) + \frac{2im}{r^2}\tilde{B}_r(r,t)\right] \\
&\quad - \left(\frac{im}{r}v_\phi + ikv_z\right)\tilde{B}_\phi(r,t) - \left(\frac{v_\phi}{r} - \frac{\partial v_\phi}{\partial r}\right)\tilde{B}_r(r,t) \\
\frac{\partial \tilde{B}_z(r,t)}{\partial t} &= \frac{1}{\mu\sigma}\left(\frac{1}{r}\frac{\partial}{\partial r}r\frac{\partial}{\partial r} - \frac{m^2}{r^2} - k^2\right)\tilde{B}_z(r,t) \\
&\quad - \left(\frac{im}{r}v_\phi + ikv_z\right)\tilde{B}_z(r,t) + \frac{\partial v_z}{\partial r}\tilde{B}_r(r,t)
\end{aligned}$$

In 2D the terms $-k^2\tilde{B}_*$ must be replaced by $\partial^2\tilde{B}_*/\partial z^2$, and a number of terms including z-derivatives and v_r-dependencies must be added. At all interfaces and boundaries the two tangential components of the electric and the normal component of the magnetic field are demanded to be continuous.

A central difference scheme is applied for the space dependent parts of both the 1D and the 2D code, with non-uniform grid spacing in the 2D case. For the outer part, in the 1D code modified Bessel functions are used and matched via the boundary conditions to the solution in the inner part. In the 2D code, for every time step the Laplace equation in the outer part is solved using a pseudo-transient method. Concerning the time dependence, the 1D code is realized as a Crank-Nicolson scheme, whereas the 2D code is realized as an explicit Adams-Bashforth method of second order. The critical Rm is determined by controlling the exponential increase or decrease of the magnetic energy.

The results were verified partly by a an older 1D code developed by one of the authors (A.G.), which uses modified Bessel functions in the various cylinders and solves the nonlinear matching equations for these Bessel functions at the inner and outer boundaries.

4. Comparison of various velocity profiles

Although a wide variety of theoretical and measured velocity profiles has been considered, we restrict ourselves in the following to five important profiles. For these profiles Table 1 shows the shape of the axial and azimuthal velocity components in the innermost cylinder[2] and the computed critical magnetic Reynolds numbers Rm^* (convective instability), Rm^{**} (absolute instability for a system with infinite length) and Rm^{***} (absolute instability for the system with finite length of the apparatus). The Rm-values are determined either by means of the above mentioned 1D eigenvalue equation solver (a) and/or the 1D time-evolution code (b) or the 2D time-evolution code (c). Additionally, Figure 1 shows the dependence of Rm^* on the parameter κ (computed with method b).

The first profile represents the solid body rotation profile (SBR), which was assumed also in former calculations. The v_z- and the v_ϕ-component of the second profile (BEF) are given by the following expressions:

$$\begin{aligned} v_z(r) &= \kappa\, J_0(2.4\, r) \\ v_\phi(r) &= 1/\sqrt{2}\, J_1(2.4\, r) \end{aligned}$$

[2]The relation between the radius R_1 of the innermost cylinder, the radius R_2 of the back-flow cylinder, the radius R_3 of the outermost cylinder and the length L of the apparatus is $R1 : R2 : R3 : L = 1.0 : 1.68 : 3.0 : 25.0$. All the profiles are assumed to be completed by a purely axial and constant back-flow. We tested also a number of back-flow profiles with azimuthal velocity components and a non-constant axial component. However, in view of the difficulties to maintain such profiles along the upward flow we considered the purely axial and constant back-flow as most appropriate for the experiment.

TABLE 1. Critical Rm for the considered velocity profiles

	SBR	BEF	NGB	WGB	PRO
v_z	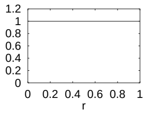	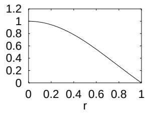	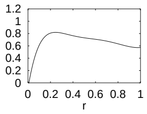	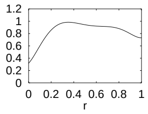	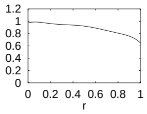
v_ϕ	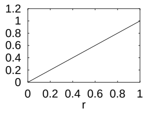	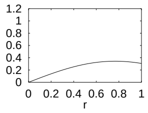	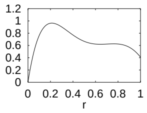	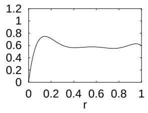	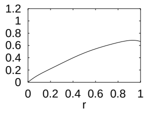
κ	1.00	1.20	0.73	1.10	1.05
Rm^*	$14.9^{a,b}$	$12.0^{a,b}$	25.6^b	17.0^b	14.2^b
Rm^{**}	$16.1^{a,b}$	$13.2^{a,b}$	26.6^b	18.3^b	15.6^b
Rm^{***}	$18.0^{a,c}$	$14.7^{a,c}$	31.0^c	21.5^c	17.5^c

Figure 1. Dependence of Rm^* on the pitch parameter κ

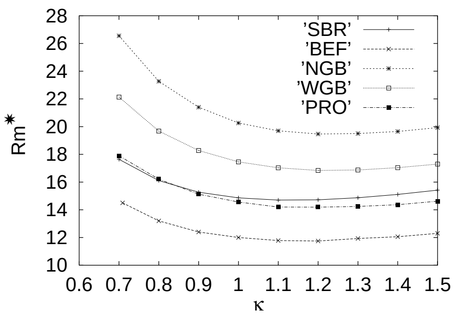

For axial symmetry, Bessel functions are well known to maximize helicity for given kinetic energy[3]. The Factor 2.4 in the argument of the modified Bessel functions is the maximal Lagrangian parameter used in the variation calculus that ensures positivity of both velocity components in the innermost cylinder. Indeed, the critical Rm-values for these helicity maximizing profiles are the lowest we were able to find. Although the minimum of Rm^* is achieved for $\kappa = 1.2$ rather than for $\kappa = 1.0$, this result underlines the important role of helicity for the dynamo effect.

The third profile was measured in a first water experiment, where only a

[3]The factor $1/\sqrt{2}$ in front of J_1 ensures (for $\kappa = 1$) helicity maximization for our somewhat "skew" expression $\overline{v_z}^2 + 2\,\overline{v_\phi}^2$.

propeller and not any guiding blades (NGB) were used[4]. All critical Rm are very large for that profile. The curve NGB in Figure 1 shows that this is in part due to the small value of the pitch parameter ($\kappa = 0.73$), but the unfavourable shape of the profile is also responsible for that. In order to avoid the undesirable over-rotation, guiding blades were welded into the upper turn-round in front of the propeller. The resulting profile (WGB) looks more favourable and yields already much lower Rm-values. The fifth profile represents a numerical prognosis (PRO) for the case that additional guiding blades are installed behind the propeller [7]. The corresponding Rm-values are a bit lower than the SBR values. If these profiles can be confirmed in the water experiment, then the self-excitation of a magnetic field in the sodium experiment should be possible.

5. Conclusions

The real shape of the velocity profiles in the Riga dynamo experiment has a serious influence on the critical magnetic Reynolds numbers. For helicity maximizing profiles Rm^* can be reduced by 20 per cent compared to the corresponding value for the solid body rotation profile. For all considered profiles, Rm^* has a minimum for κ close to 1.1. Thus, high helicity and a suitable pitch parameter are both important for the optimization of the velocity profiles.

Acknowledgments

This work was supported by Deutsche Forschungsgemeinschaft under INK 18/A1-1.

References

1. Ponomarenko, Yu. B. (1973) On the theory of hydromagnetic dynamos, *Zh. Prikl. Mekh. Tekhn. Fiz.,* **6**, 47-51
2. Gailitis, A.K., Karasev, B.G., Kirillov, I.A., Lielausis, O.A., Luzhanskii, S.M., Ogorodnikov, A.P., Preslitskii, G.V. (1987) Liquid metal MHD dynamo model experiment, *Magnitnaya Gidrodinamika* **4** 3-7
3. Gailitis, A. (1996) Project of a liquid sodium MHD dynamo experiment *Magnitnaya Gidrodinamika* **32** 63-67
4. Stieglitz, R., Müller, U. (1996) GEODYNAMO - Eine Versuchsanlage zum Nachweis des homogenen Dynamoeffektes, FZKA 5716
5. Christen, M. (1996) private communication
6. Gailitis, A. K., Freiberg, J. ZH. (1977) Calculation of helical flux dynamo-instability, Preprint Riga
7. Christen, M. (1997) private communication

[4]The measurements were carried out by means of a pressure probe in march 1997. It should be noted that the measured values close to the axis might be not very reliable [7].